Supporting Information

Acene-Based Organic Semiconductors for Organic Light-Emitting Diodes and Perovskite Solar Cells

Hong Duc Pham,[a♦] Hongwei Hu,[b♦] Fu-Lung Wong,[c♦] Chun-Sing Lee,[c] Wen-Cheng Chen,[c] Krishna Feron,[d,e] Sergei Manzhos,[f] Hongxia Wang,[a] Nunzio Motta,[a] Yeng Ming Lam,[b] Prashant Sonar[a*]

[a] Institute of Future Environment and School of Chemistry, Physics and Mechanical Engineering, Queensland University of Technology (QUT), 2 George Street, Brisbane, QLD-4001, Australia.

[b] School of Materials Science and Engineering, Nanyang Technological University, 50 Nanyang Avenue, 639798, Singapore.

[c] Center of Super-Diamond and Advanced Films, City University of Hong Kong, Kowloon, Hong Kong, P. R. China.

[d] CSIRO Energy Centre, NSW-2304, Australia.

[e] Centre for Organic Electronics, University of Newcastle, Callaghan, NSW 2308, Australia

[f] Department of Mechanical Engineering, Faculty of Engineering, National University of Singapore, Block EA #07-08, 9 Engineering Drive 1, Singapore 117576.

Experimental details:

Materials and Instruments:

All chemicals and reagents were purchased from commercial vendors and used directly without any further purification. Reactions were monitored by thin layer chromatography (TLC) and were carried out under argon atmosphere.

^{1}H and ^{13}C NMR spectra were performed on a Bruker 600 MHz spectrometer. High-resolution mass spectra were acquired on an LTQ Orbitrap Elite mass spectrometer (Thermo Fisher Scientific, Bremen, Germany) equipped with an electrospray ionisation (ESI) source, operating in the positive ion mode at a resolution of 120,000 (at *m/z* 400). Reserpine ($[M+H]^+$, *m/z* 609.28066) was used as a lockmass calibrant to increase the measurement accuracy. UV-Vis spectra were recorded on a Shimadzu UV-1800 spectrometer. Differential-scanning-calorimetry (DSC) was performed using a Q100 DSC Chimaera equipped with a cooling apparatus. The thermogravimetric analysis (TGA) was performed using a Q500TGA Pegasus. Photoelectron spectroscopy in air (PESA) measurements was conducted using on an AC-2 photoelectron spectrometer (Riken-Keiki Co.).

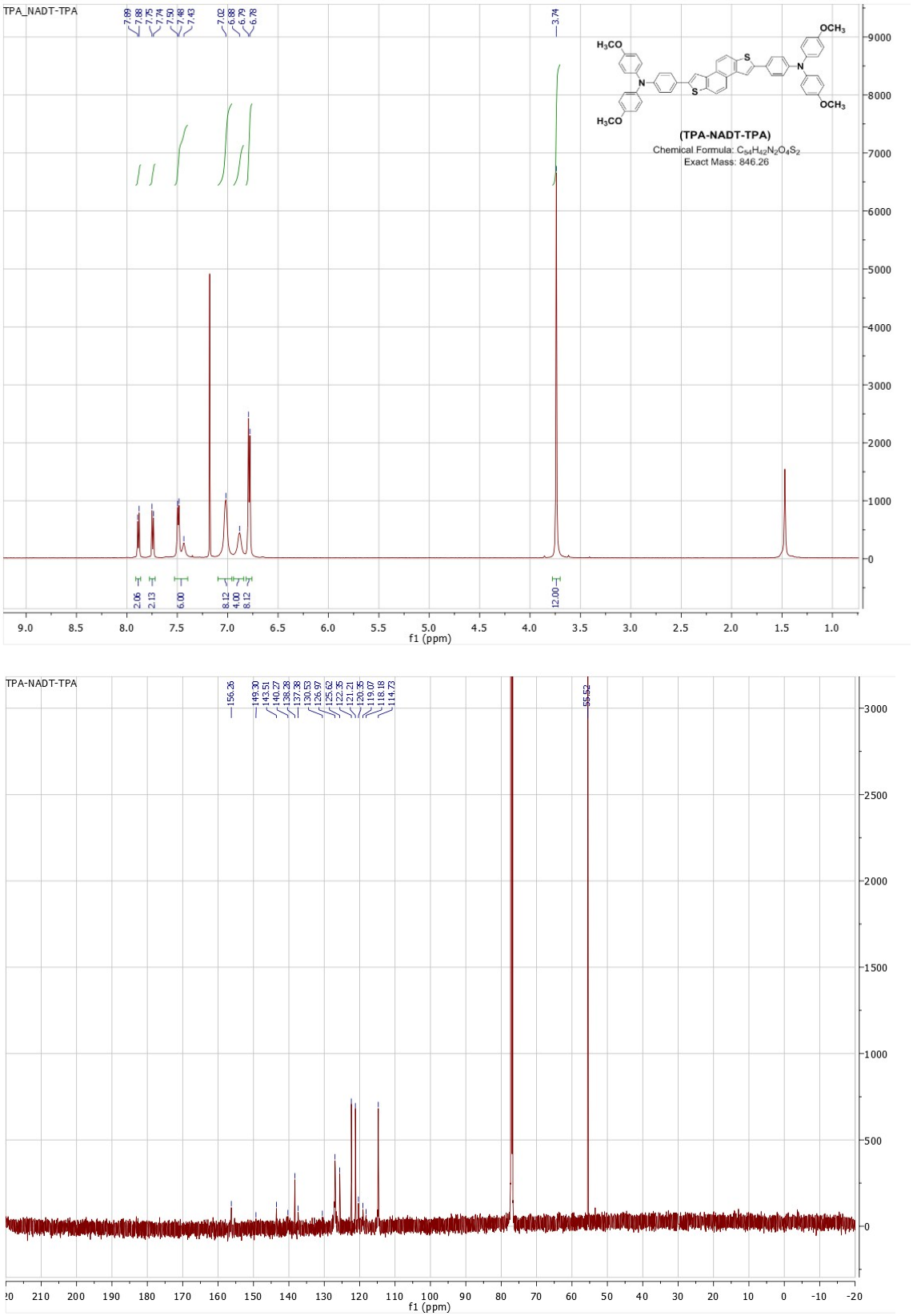

Fig. S1. (a) ^{1}H (600 MHz, $CDCl_3$) spectrum and (b) ^{13}C NMR (120 MHz, $CDCl_3$) spectrum of (**TPA-NADT-TPA**).

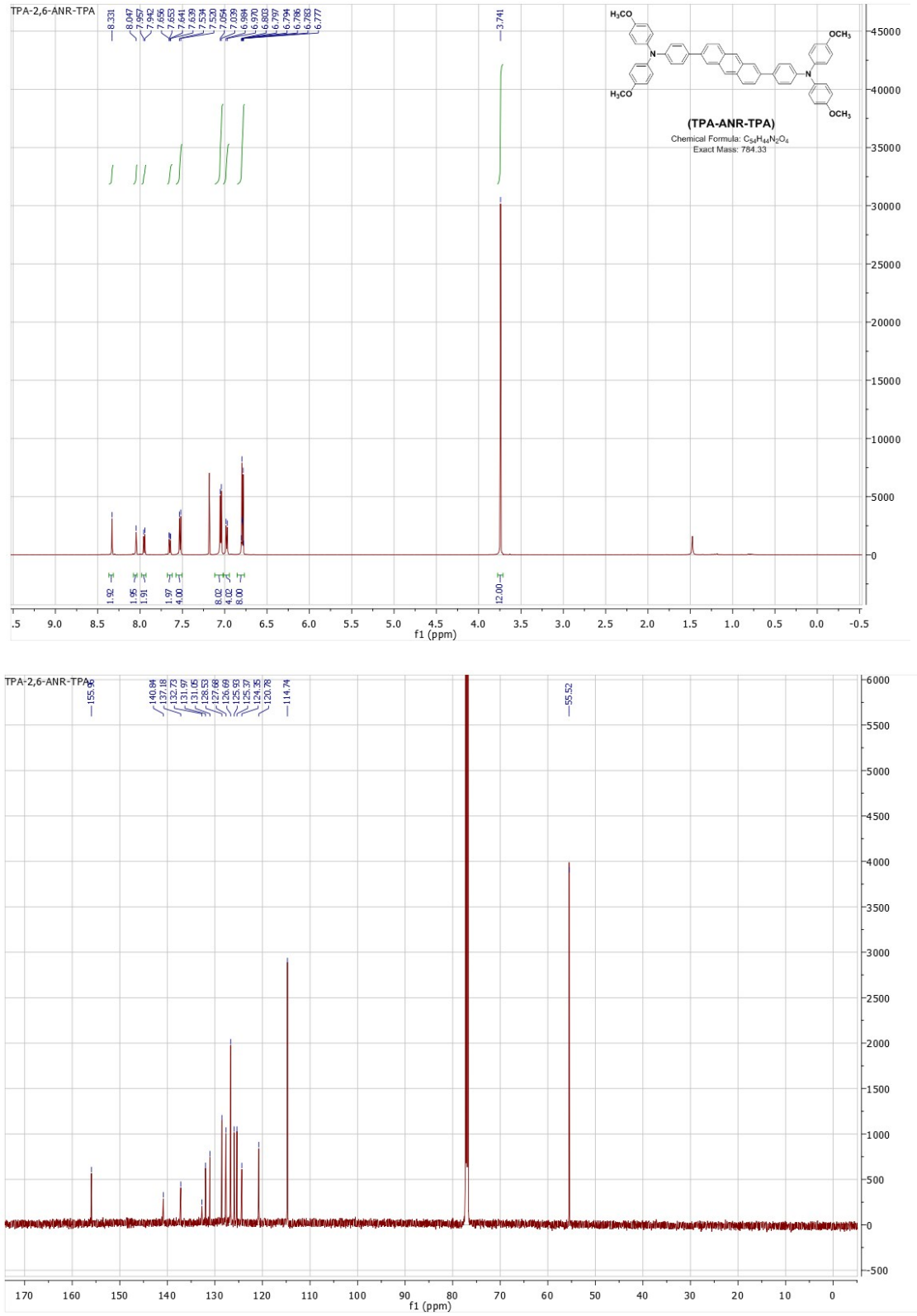

Fig. S2. (a) ^{1}H (600 MHz, $CDCl_3$) spectrum and (b) ^{13}C NMR (120 MHz, $CDCl_3$) spectrum of (**TPA-ANR-TPA**).

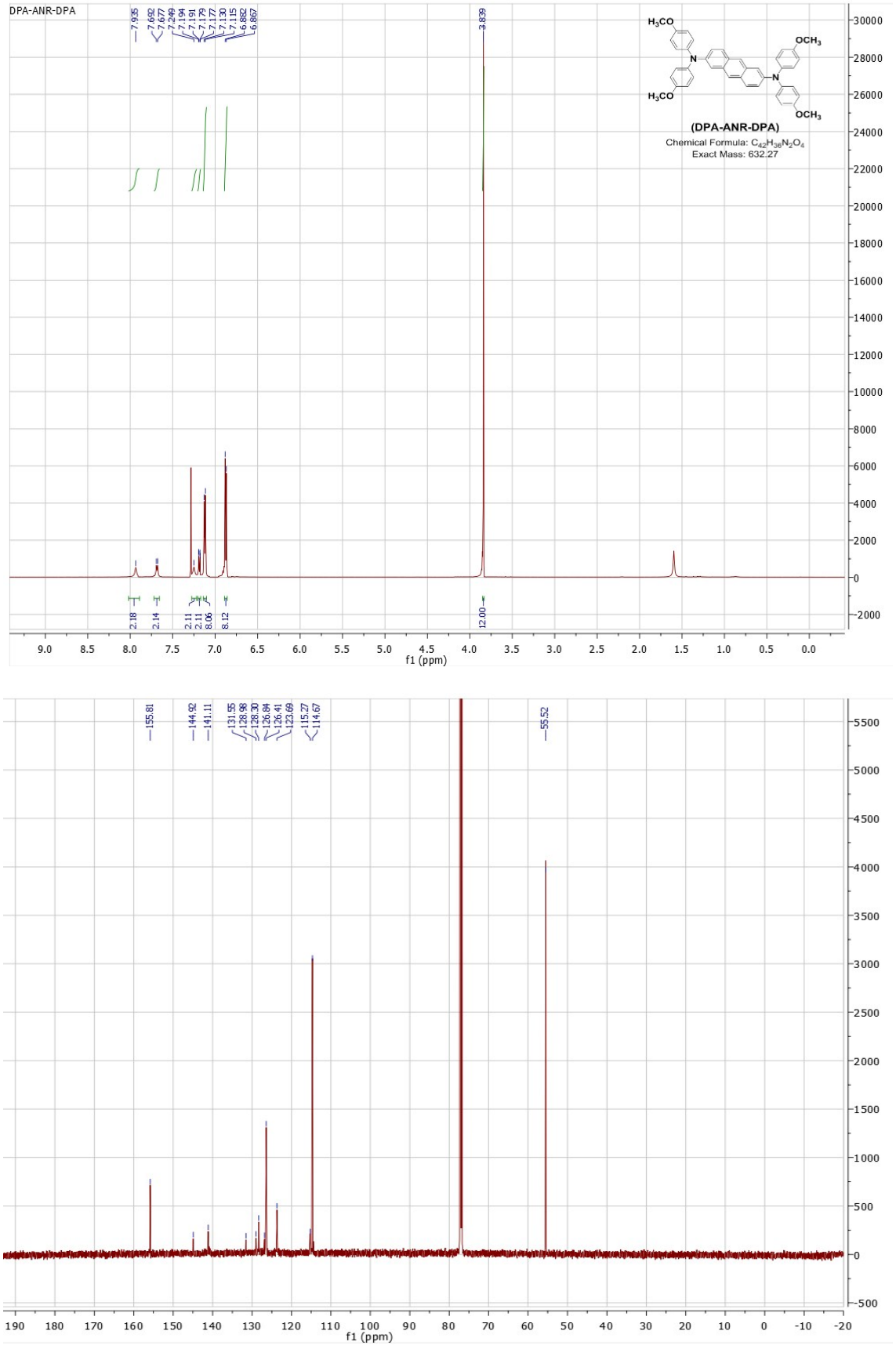

Fig. S3. (a) ^{1}H (600 MHz, $CDCl_3$) spectrum and (b) ^{13}C NMR (120 MHz, $CDCl_3$) spectrum of (**DPA-ANR-DPA**).

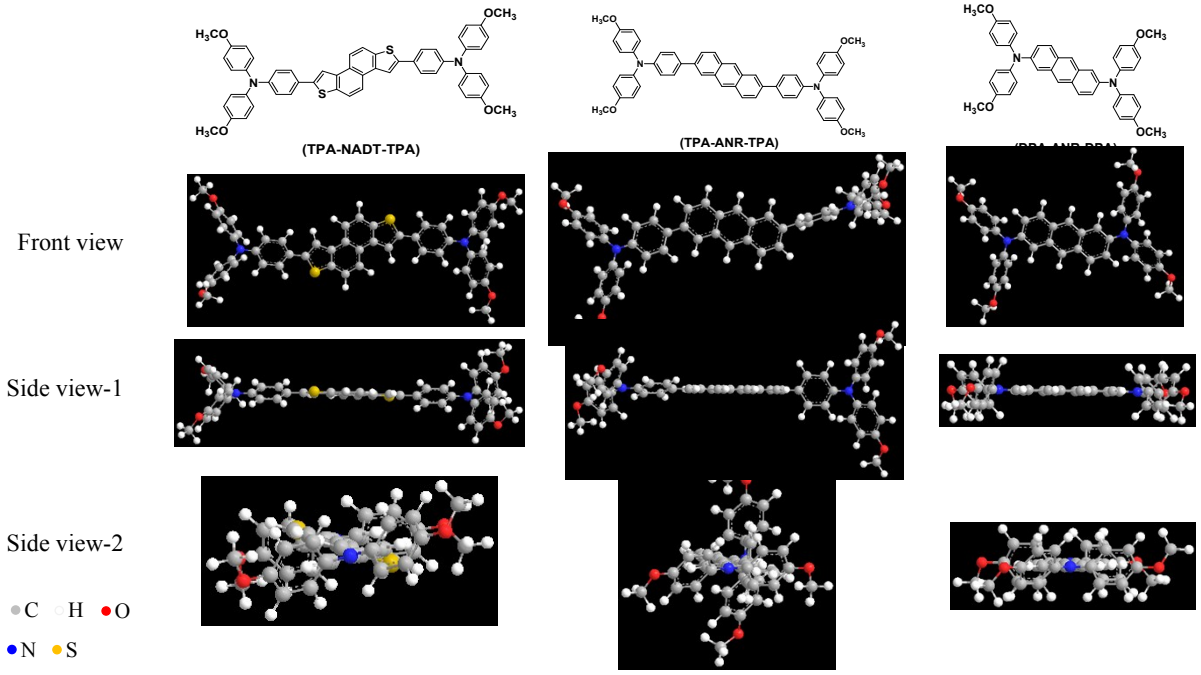

Fig. S4. Chemical structures and front-side views of the geometry of (left to right) TPA-NADT-TPA, TPA-ANR-TPA, and DPA-ANR-DPA.

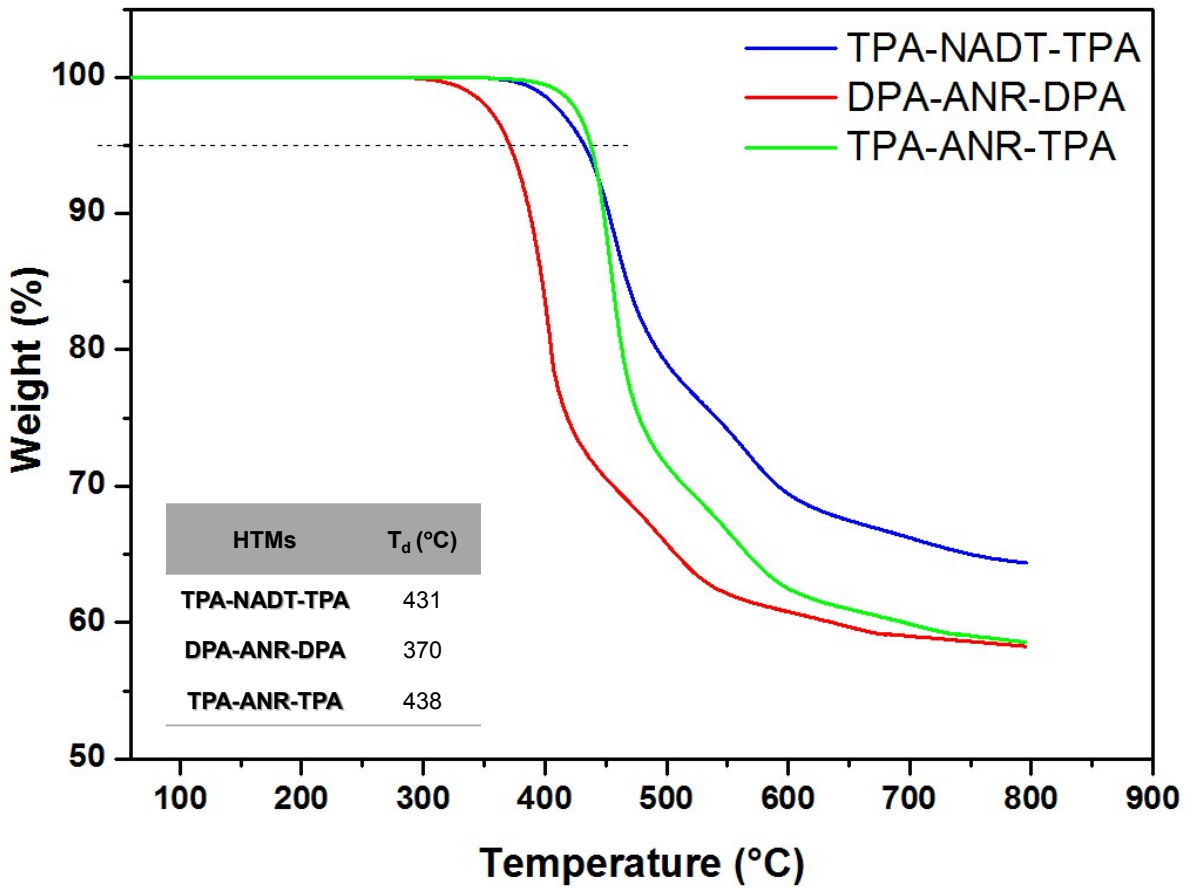

Fig. S5. Thermogravimetric analysis (TGA) curve of three new materials.

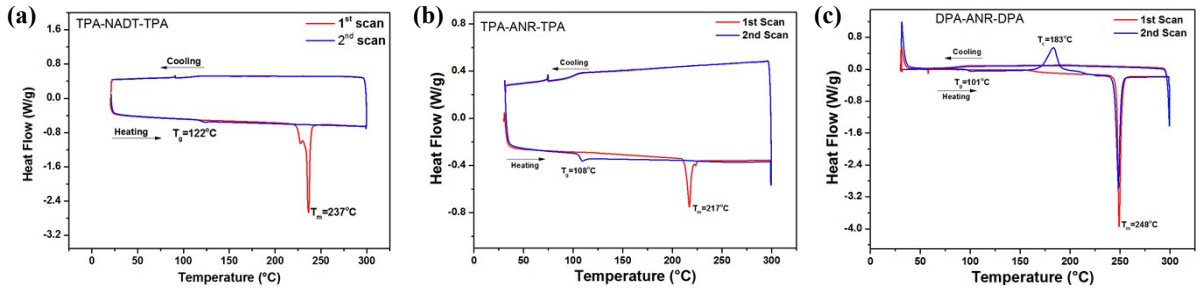

Fig. S6. Differential scanning calorimetry (DSC) of (a) TPA-NADT-TPA, (b) TPA-ANR-TPA and (c) DPA-ANT-DPA with scan rate of 10 °C/min under N_2 atmosphere.

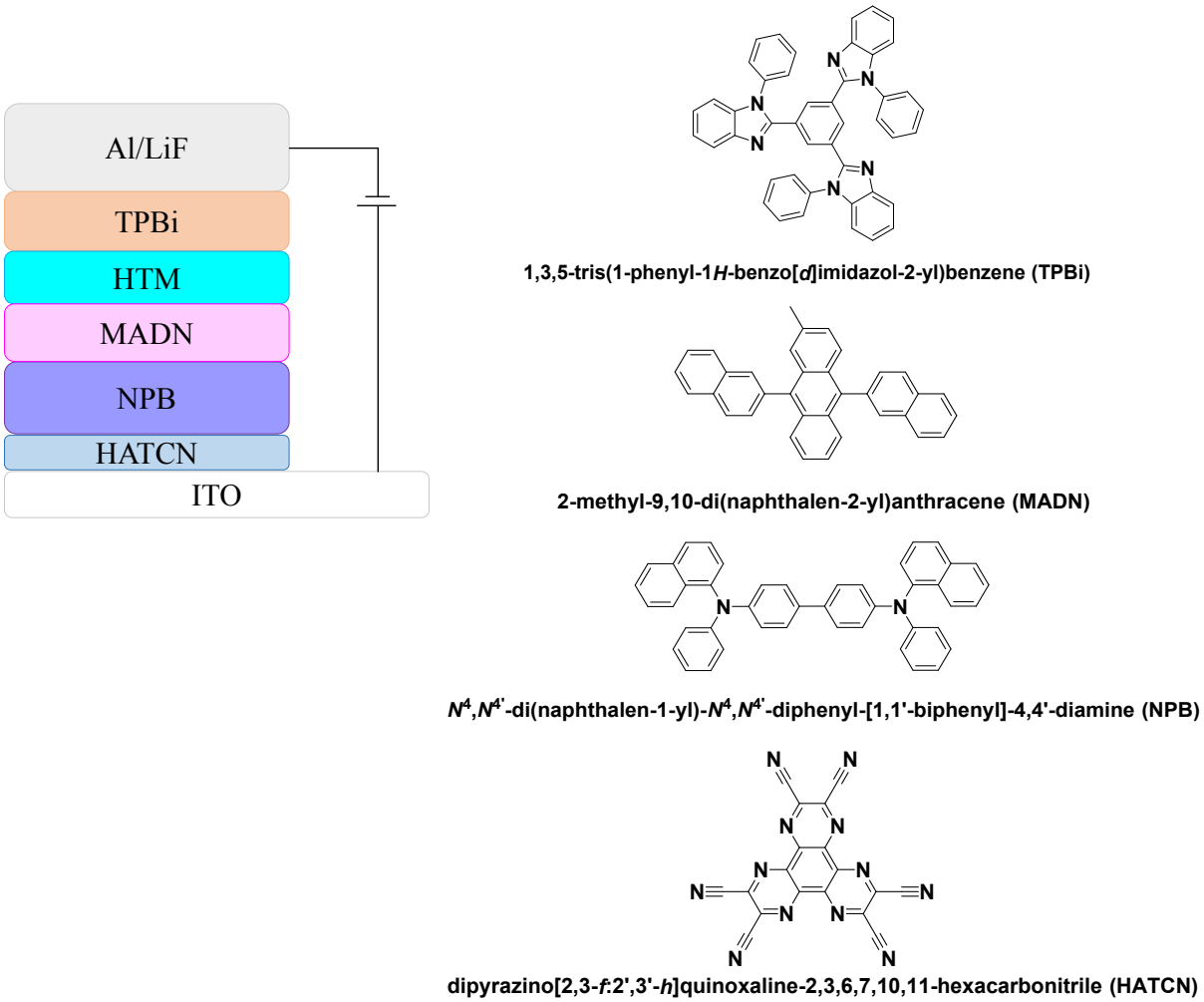

Fig. S7. The structures of molecules used in OLED devices. The device architecture is shown on the left.

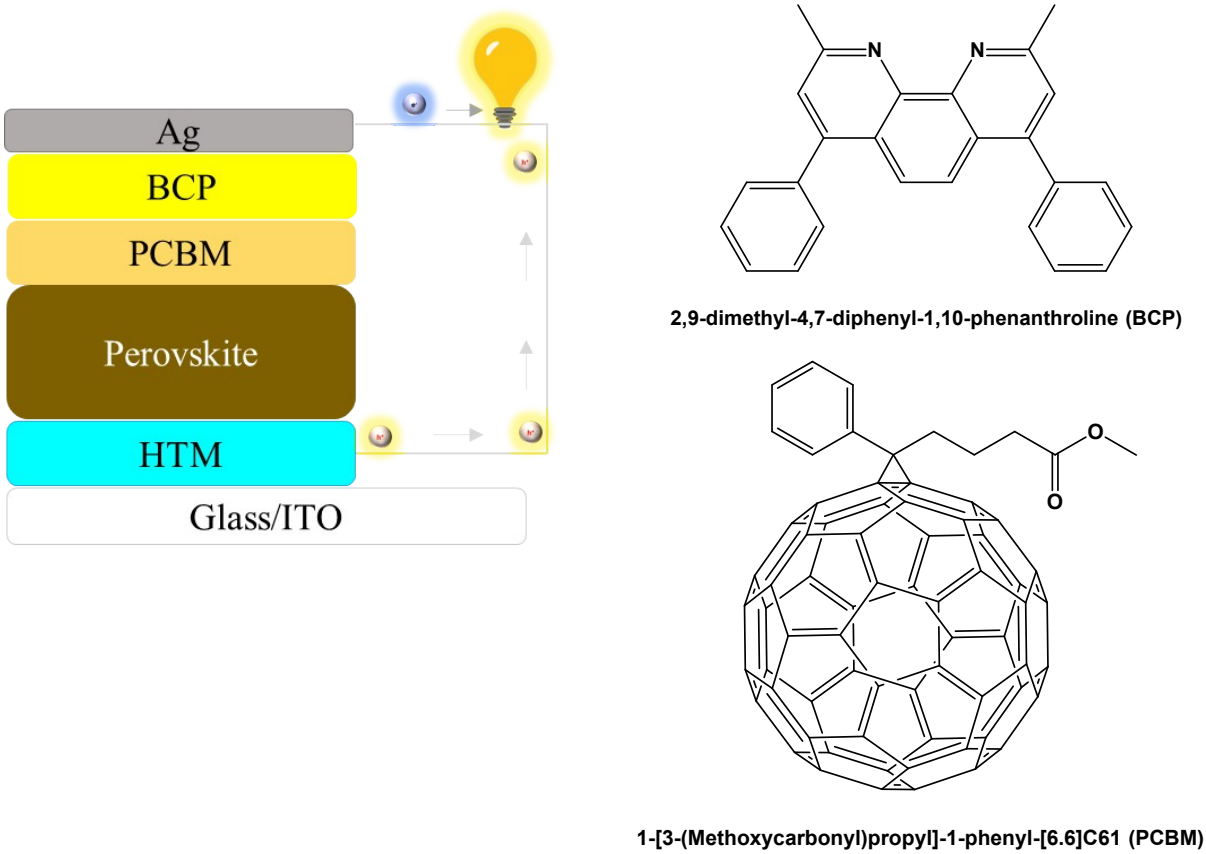

Fig. S8. The structures of molecules used in PSC devices. The device architecture is shown on the right.

Table S1. Density Functional Theory (DFT) and Time-Dependent DFT (TD-DFT) calculations of TPA-NADT-TPA, TPA-ANR-TPA and DPA-ANR-DPA.

Compound	TPA-NADT-TPA	TPA-ANR-TPA	DPA-ANR-DPA
HOMO, eV	-4.90	-4.84	-4.68
LUMO, eV	-1.90	-2.03	-1.83
gap, eV	3.00	2.81	2.85
VIS peak(s), nm	476.6	502.02	510.6
osc strength	1.8087	0.7928	0.3383
composition	H→L	H→L	H→L
PL peak(s), nm	554.4	577.2	596.3
osc strength	1.9156	1.0601	0.3383
composition	H→L	H→L	H→L
dihedrals TPA-core	5.4	28.5	n/a